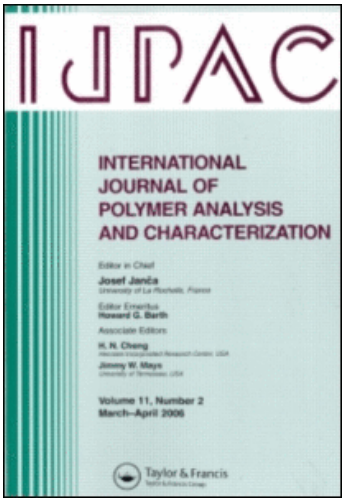

International Journal of Polymer Analysis and Characterization
Publication details, including instructions for authors and subscription information:
http://www.informaworld.com/smpp/title~content=t713646643

Continuous Monitoring of the Effect of Changing Solvent Conditions on Polyelectrolyte Conformations and Interactions

Erica E. Bayly[a]; Jean-Luc Brousseau[a]; Wayne F. Reed[a]
[a] Physics Department, Tulane University, New Orleans, Louisiana, USA

Online publication date: 27 October 2010

To cite this Article Bayly, Erica E. , Brousseau, Jean-Luc and Reed, Wayne F.(2002) 'Continuous Monitoring of the Effect of Changing Solvent Conditions on Polyelectrolyte Conformations and Interactions', International Journal of Polymer Analysis and Characterization, 7: 1, 1 — 18
To link to this Article: DOI: 10.1080/10236660214596
URL: http://dx.doi.org/10.1080/10236660214596

International Journal of Polymer Anal. Charact., 7: 1–18, 2002

1023-666X/02 $12.00+.00

Continuous Monitoring of the Effect of Changing Solvent Conditions on Polyelectrolyte Conformations and Interactions

Erica E. Bayly, Jean-Luc Brousseau, and Wayne F. Reed
Physics Department, Tulane University, New Orleans, Louisiana, USA

This work introduces a technique for the continuous, automatic determination of the response of polyelectrolytes to changing solution conditions. Using a ternary pump to automatically change the solvent character for polyelectrolyte solutions, it is possible to continuously measure the changes in polyelectrolyte conformations and interactions. Detection is accomplished with a series of detectors, including multiangle light scattering, a single-capillary viscometer and a refractive index detector. The technique is applied to the ionic strength behavior of stiff, semiflexible and flexible polyelectrolytes. The effects of possible ion specificity and a quantitative comparison to current polyelectrolyte theories is left to future work.

Keywords: Polyelectrolyte; Light scattering; Viscometry; Conformation; Xanthan; Hyaluronic acid; Poly(styrenesulfonate)

Received 31 May 2000; accepted 8 September 2000.
The authors gratefully recognize support from NSF CTS 9877206 and La. BoR RD-B-11. J.L.B. acknowledges support from Elf Atochem Corp.
Address correspondence to Wayne F. Reed, Department of Physics, Tulane University, New Orleans, LA 70118.

A large body of work has accumulated concerning the response of polyelectrolytes to changing solvent conditions, especially those involving ionic strength. It is beyond the scope of this work to give a comprehensive survey of the literature. Treatments of electrostatic persistence lengths and excluded volume and their relation to polyelectrolyte conformations and interactions were first made by Odijk[1,2], Skolnick and Fixman[3,4]. Because precise analytical solutions to the excluded volume problem do not exist, there have also been computer simulation approaches[5–9]. A general review of polyelectrolytes was given recently by Förster and Schmidt[10].

Experimental characterization of polyelectrolytes under changing solution conditions has traditionally been tedious and fraught with inconsistencies. Viscosity, static and dynamic light scattering[11] have figured prominently in characterization efforts. At extremely low ionic strength, qualitative differences in behavior occur. For example, there is a maximum in reduced viscosity vs. polyelectrolyte concentration when a very low ionic strength polyelectrolyte solution is diluted with a solvent of low, constant ionic strength[12–15]. Both neutron and static light scattering have revealed broad scattering maxima for such solutions[16–19]. Dynamic light scattering of low ionic strength polyelectrolyte solutions has frequently revealed a slow diffusional mode[20–22], although this has been attributed by some to the presence of incompletely dissolved aggregates, which can be removed by filtration[23–26].

In order to increase the quality, scope and resolution of polyelectrolyte characterization data, and to ease the labor involved, a continuous, automated technique is introduced here. The purpose of this work is to introduce the technique and present initial results. A quantitative comparison with current polyelectrolyte theory is left to future work being planned, where even higher resolution data will be obtained on a more exhaustive set of conditions. The technique should be amenable to a wide variety of other experiments in which complex interactions among polyelectrolytes, neutral polymers, colloids, etc., are of interest.

MATERIALS AND METHODS

The Continuous Dilution Technique

Florenzano et al.[27] introduced the use of continuous automatic dilution with a binary mixing pump for online monitoring of polymerization reactions. It was later employed by Strelitzki and Reed[28] for automatic, continuous characterization of polymers using both light

scattering and viscosity detectors. The traditional use of mixing pumps in separation science has been to achieve solvent gradients in liquid chromatography to separate molecules according to polarity, specific adsorption and other effects. The use of mixing pumps for nonseparation purposes to characterize both equilibrium and nonequilibrium properties of polymers and colloids appears to be new.

In this work a ternary programmable mixing pump (ISCO 2360, Lincoln, Nebraska) is used so that solvent quality can be changed continuously, while the polyelectrolyte concentration is held constant. To achieve this, a stock concentration of polyelectrolyte is prepared in a chosen solvent, pure water in this case, and is pumped at a fixed percentage (10%) of the total mix from reservoir A. Reservoir B contains pure water. Reservoir C contains the aqueous solvent at high ionic strength (typically around 60 mM). During the experiment the percentage from reservoir B gradually decreases from 90% to 0%, and that of C increases from 0% to 90%, so that the effect on the polyelectrolyte of all ionic strengths between 0% and 90% of the ionic strength in C are monitored. Again, the concentration of the polyelectrolyte throughout the experiment is held constant by withdrawing a fixed 10% from A. At every instant the inlets from reservoirs A, B, and C are continously mixed by the pump and delivered to the detector string. The contents of the mixing chamber are continuously withdrawn and pumped through the detector train by an ISCO 2350 isocratic pump.

For these experiments the detectors consisted of a laboratory-built multiangle (seven angles spanning 33°–144°) light scattering chamber (LS) previously described[28], a single-capillary viscometer, also previously described[29], and a Waters 410 refractometer (RI). Since the concentration of the polyelectrolyte is known and held constant throughout the experiment, the LS suffices to determine the z-average root-mean-square radius of gyration $\langle S^2 \rangle_z$, and the second virial coefficient A_2. The RI is needed, however, to monitor the composition of the solvent at every instant. For NaCl the value of dn/dc was determined to be 0.174 cm^3/g. The viscometer provides an independent signal directly proportional to the solution viscosity, which is simply related to the reduced polymer viscosity, as explained below. The flow rate was 1.0 mL/min. All experiments were performed at room temperature.

Data Evaluation

The well-known Zimm approximation[30] allows determination of weight-average molecular mass M_w, second and third virial coefficients A_2 and A_3, respectively, and particle shape factor $P(q)$. Zimm has shown, that to 2nd order in concentration c (g/cm^3), the quantity $Kc/I(q, c)$,

where $I(q,c)$ is the excess Rayleigh scattering ratio, can be approximated by

$$\frac{Kc}{I(q,c)} = \frac{1}{MP(q)} + 2A_2c + [3A_3Q(q) - 4A_2^2\mathrm{MP}(q)(1-P(q))]c^2 \qquad (1)$$

where $Q(q)$ approaches 1 in the low angle limit. This equation forms the basis of the well-known Zimm plot, which, at low concentrations and for $q^2\langle S^2\rangle \ll 1$ can be written, for a polydisperse polymer population as

$$\frac{Kc}{I(q,c)} = \frac{1}{M_w}\left(1 + \frac{q^2\langle S^2\rangle_z}{3}\right) + 2A_2c \qquad (2)$$

which directly permits determination of M_w, A_2 and the z-average mean-square-radius of gyration $\langle S^2\rangle_z$. K is an optical constant, given for vertically polarized incident light by

$$K = \frac{4\pi^2 n^2 (\mathrm{d}n/\mathrm{d}c)^2}{N_A\lambda^4} \qquad (3)$$

where n is the solvent index of refraction, λ is the vacuum wavelength of the incident light, $\mathrm{d}n/\mathrm{d}c$ is the differential refractive index for the polymer in the chosen solvent, and q is the usual scattering wave-vector $q = (4\pi n/\lambda)\sin(\theta/2)$, where θ is the scattering angle.

For the case of polyelectrolytes being subjected to changing ionic strength, the M_w does not change. Hence, as long as M_w is known, and as long as the dilution and angular limit where equation (2) applies, $\langle S^2\rangle_z$ and A_2 can be determined by

$$\langle S^2\rangle_z = 3M_w\frac{\mathrm{d}[Kc/I(q,c)]}{\mathrm{d}q^2} \qquad (4)$$

and

$$A_2 = \frac{1}{2c}\left[\frac{Kc}{I(0,c)} - \frac{1}{M_w}\right] \qquad (5)$$

For random coils at higher values of $q^2\langle S^2\rangle_z$, where, equations (2) and (4) no longer apply, the Debye function for ideal coils has an asymptote such that a value of 2 replaces the value of 3 in those equations. Equation (5) will continue to hold in the dilute solution limit since it is independent of q, except in the extremely low ionic strength limit where strong interparticle correlations might exist (discussed below).

Total solution viscosity is given by

$$\eta = \eta_s[1 + [\eta]c + k_p[\eta]^2c^2] \qquad (6)$$

where η_s is the pure solvent viscosity, $[\eta]$ is the intrinsic viscosity of the polymer and k_p is a constant related to the hydrodynamic interactions between polymer chains, usually around 0.4 for neutral, random coil polymers[31]. The intrinsic viscosity $[\eta]$ is the extrapolation to zero concentration and zero shear rate of the reduced viscosity η_r. The value of η_r can be computed directly from the voltage of a single-capillary viscometer (a differential pressure transducer) at every point i, without need of an instrumental calibration factor, in terms of the viscometer baseline voltage V_b, and the concentration at point i, c_i

$$\eta_{r,i} = \frac{V_i - V_b}{c_i V_b} \tag{7}$$

This is so because the output of the viscometer is directly proportional to the pressure drop across the capillary of radius R and length L, which in turn is directly proportional to the total solution viscosity via Poisseuille's equation

$$\eta = \frac{\pi R^4 P}{8LQ} \tag{8}$$

where Q is the flow rate through the capillary (in cm^3/s). The average shear rate in the capillary is

$$\dot{\gamma}_{ave} = \frac{8Q}{3\pi R^3} \tag{9}$$

In the method presented here the average shear rate is about $860\,s^{-1}$ for $Q = 1.0\,mL/min$ and $R = 0.0254\,cm$. Fortunately, shear effects diminish with diminishing c. It is also noted that it is currently standard practice in size exclusion chromatography (SEC) coupled to viscometric detectors to approximate $[\eta]$ by the values of η_r determined at finite (but low) c and finite shear rate.

Polyelectrolytes

Hyaluronic acid (HA from *streptococcus zooepidemicus*) was from Sigma (St. Louis, Missouri), xanthan was a gift of SKW Biosystems S.A (Baupte, France) and poly(styrenesulfonate) (PSS) was from American Polymer Laboratories (Mentor, Ohio). Distilled, deionized water of conductivity less than 0.05 μS was provided from a Modulab Water Purification System (Bedford, Massachusetts). Polyelectrolytes were dissolved directly in this water, stirred at low speed for typically four hours, then filtered through either a 0.22-μm or 0.45-μm Millipore GS filter. It was previously found via real-time observations of polyelectrolyte dissolution[26] that this is more than sufficient time for dissolution, and that the filtration is sufficient to remove any incompletely dissolved polyelectrolyte aggregates that can persist for long periods.

TABLE I SEC Characteristics of xanthan and hyaluronic acid in 0.1 M NH_4NO_3. The poly(styrenesulfonate) M_w used was the nominal value of supplier (2.85×10^6 g/mol).

Sample	M_w (10^6 g/mol)	η_{red}(cm^3/g)	$\langle S^2 \rangle_z^{1/2}$ (Å)	$\langle S^2 \rangle_w^{1/2}$ (Å)
Hyaluronic acid	1.50	2940	1400	1370
Xanthan	1.45	1900	1440	1370

Table I gives an SEC analysis, using SEC apparatus previously described[32] for HA and xanthan samples.

RESULTS AND DISCUSSION

Figure 1 shows the combined raw LS (at one of the seven angles), viscometer and RI responses vs. time for a typical experiment for HA

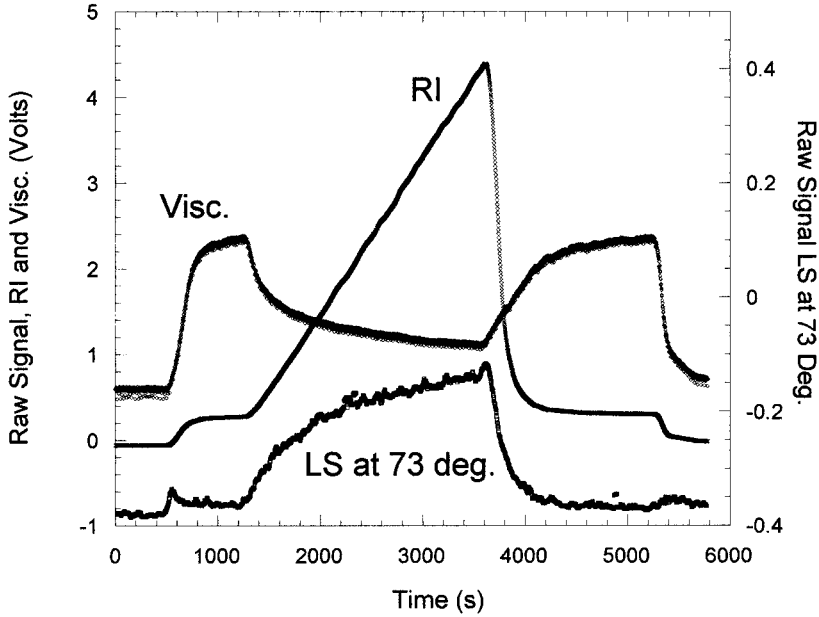

FIGURE 1 Combined LS (at one of seven angles), viscometer and RI responses vs. time for a typical experiment for hyaluronic acid at a fixed concentration of 0.00041 g/mL.

at 0.00041 g/mL. Up to about 500 s, 100% pure water is pumped from reservoir B, after which 0.00041 g/mL HA in pure water was introduced by pumping 10% of the 0.0041 g/mL HA stock in reservoir A and 90% pure water from B. The pure water signals up to 500 s provided the baselines for subsequent computations of Kc/I and reduced viscosity. At about 1150 s the ionic strength gradient began. This involved programming the pump to pass from 90% of B to 0% of B, while the concentration from the high ionic strength solution in C went from 0 to 90%. The withdrawal of HA from A throughout the entire experiment remained at 10%, ensuring constant HA concentration.

As expected, the scattering intensity begins to rise as ionic strength increases, due to electrostatic screening and consequent reduction in A_2, whereas viscosity decreases as the HA polymer coil contracts with increasing salt. At about 3600 s the solvent was returned to HA solution in pure water (10% A, 90% B, 0% C), and then at about 5300 s it was returned to pure water (100% B). It is seen that the viscosity and scattering signals return to the level they were at just before the concentration gradient began. The increase in scattering intensity as ionic strength increases due to the decrease in the electrostatic contribution to A_2 is a well-known effect. In this and subsequent experiments, the increase in both light scattering and solvent viscosity due to the relatively low level of added salt (up to 59 mM) is negligible compared to the large scattering and viscosity signals from the polyelectrolyte itself.

Figure 2 shows the data from Figure 1 vs. added NaCl concentration (mM), which is a more relevant representation for analyses in terms of polyelectrolyte theories. All signals are nearly at a plateau by about 75 mM NaCl, indicating that only relative small effects would occur if ionic strength were raised further. It is noted that in this and subsequent raw data figures the light scattering voltage at each angle is unnormalized, i.e., its voltage value cannot be directly compared with the other angles. Naturally, in analyzing the data, the voltage signals at each angle are normalized in the usual fashion (e.g., References [27, 28, 32]).

Figure 3 shows raw data for xanthan vs. [NaCl], and Figure 4 shows raw data for PSS vs. [NaCl]. The xanthan reaches plateaus in scattering and viscosity at about 10 mM NaCl, a much lower concentration than for HA, which in turn achieves these plateaus at lower [NaCl] than PSS. This is a direct indication of the relative flexibilities.

Figure 5 shows the reduced viscosities for PSS, HA and xanthan on a single curve. The xanthan shows no change in η_r beyond about 5 mM salt. The limiting value of $1950 +/-50$ is in excellent agreement with the SEC result in Table I. This is also in good agreement with the value reported by Milas et al., for xanthan of similar size[33]. The HA value at

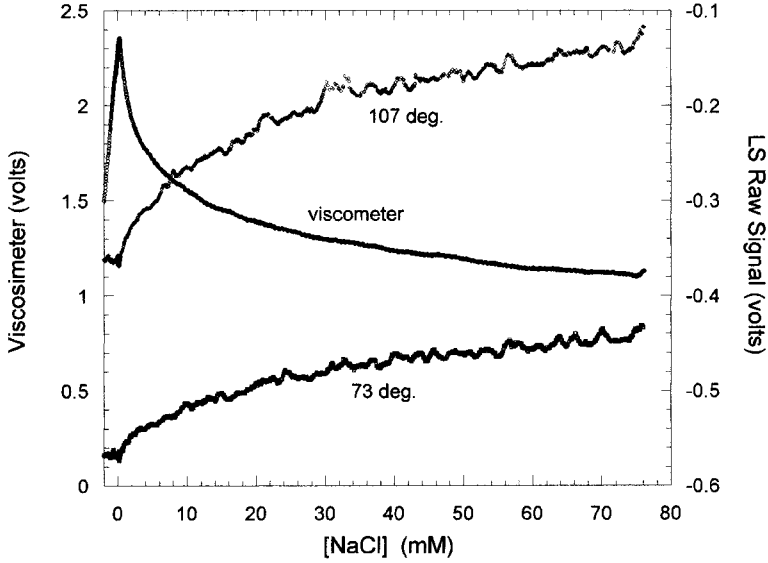

FIGURE 2 The data from Figure 1 vs. added NaCl concentration (mM), where the [NaCl] concentration is determined from the RI signal.

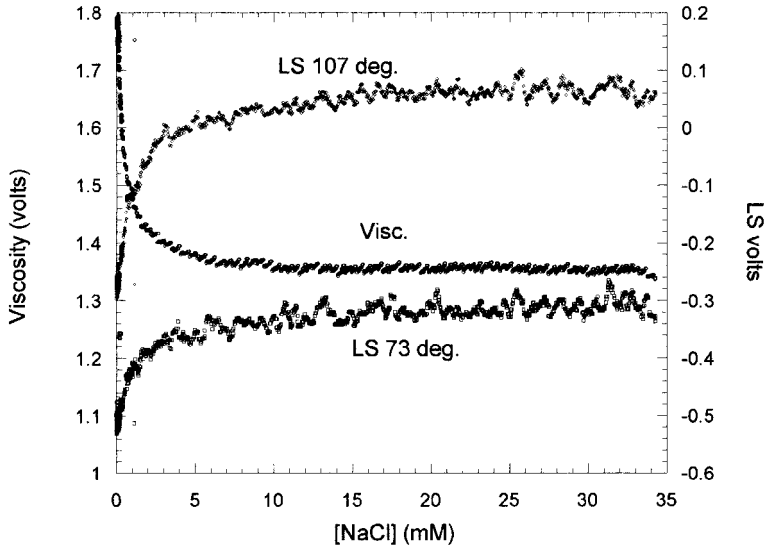

FIGURE 3 Raw LS (at 73° and 107°) and viscosity data for xanthan at a fixed concentration of 0.00040 g/mL vs. [NaCl], which varied from 0 to 35 mM.

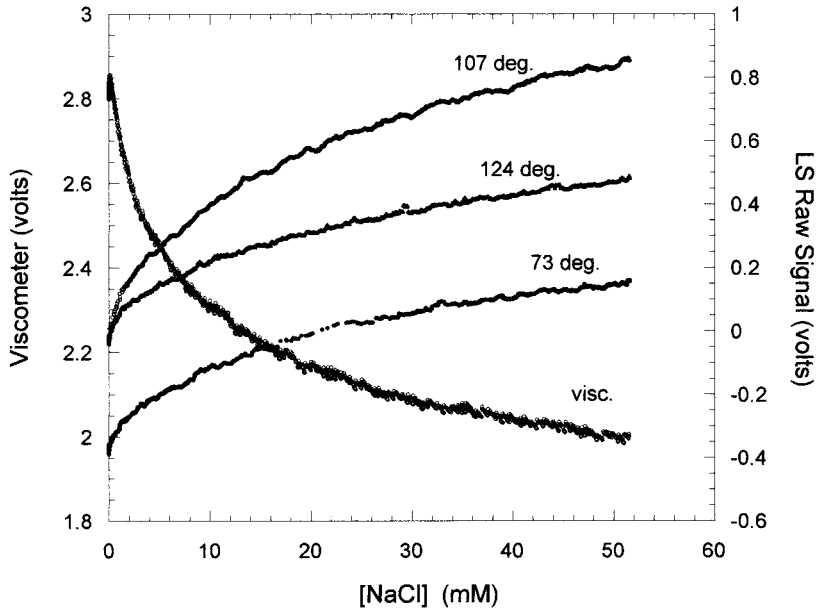

FIGURE 4 Raw LS (for three angles) and viscosity data for poly(styrenesulfonate) at a fixed concentration of 0.00041 g/mL vs. [NaCl], which varied from 0 to 52 mM.

high [NaCl] on Figure 5 is about 2200, which is in fair agreement with the SEC data in Table I. Figure 6 shows the reduced viscosities for PSS, HA and xanthan on a single curve, scaled to a single initial value, to illustrate the difference in flexibilities of each. Figure 7 shows raw light scattering at 73° for the three polyelectrolytes on one graph. Again, the relative flexibilities can be seen by the rate at which they approach their respective light scattering plateaus. Figure 8 shows the extrapolation of Kc/I to $q=0$ for PSS and xanthan. From this, under the dilute solution approximation of equation (5), A_2 can be determined as a function of [NaCl], which is shown in Figure 9, for all three polyelectrolytes. The values are in reasonable agreement with previous reports at discrete ionic strengths for HA[34] and PSS[35]. Further work will include continuous variation of polyelectrolyte concentration at discrete ionic strenghts in order to ascertain both values of A_3, and over what concentration ranges it is sufficient to use simply A_2, as well as assessments of A_2 variations in light of combined theories of electrostatic persistence length and excluded volume[11].

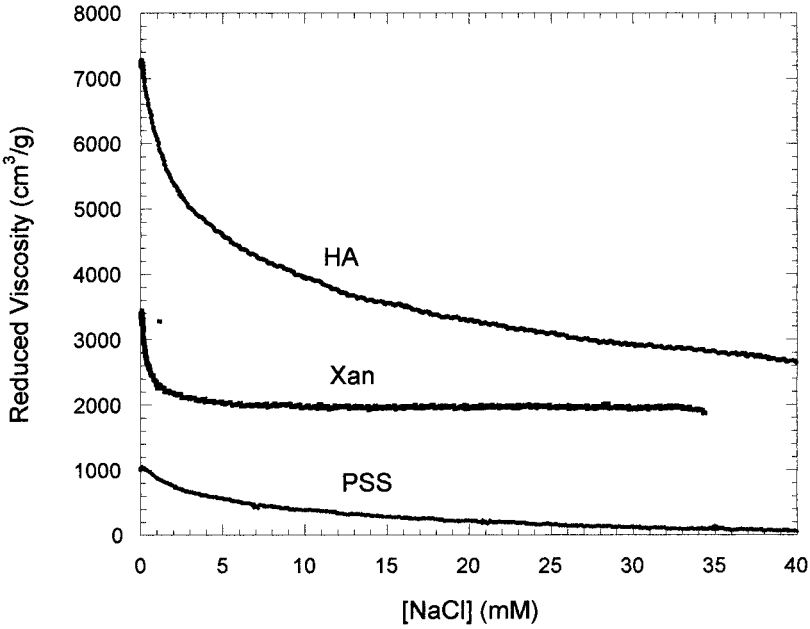

FIGURE 5 Reduced viscosities for poly(styrenesulfonate), hyaluronic acid and xanthan on a single curve. All polyelectrolyte concentrations are the same as above in this and subsequent figures.

The wormlike chain formula, which spans conformations from random coil molecules at theta conditions to fully extended rods, is given by[36]

$$\langle S^2 \rangle_\theta = \frac{LL_T}{3} - {L_T}^2 + \frac{2{L_T}^3}{L} - 2\frac{{L_T}^4}{L^2}\left[1 - \exp\left(-\frac{L}{L_T}\right)\right] \qquad (10)$$

where L is the contour length of the polymer, L_T the persistence length, and $\langle S^2 \rangle_\theta$ is the mean-square radius of gyration measured under theta conditions. Because local electrostatic chain stiffening and excluded volume effects are virtually impossible to separate experimentally, the above relation has sometimes been employed in good solvent (non-theta) conditions, using the measured $\langle S^2 \rangle_z$, and the persistence length thus obtained is termed the apparent persistence length, L_T[9].

Figure 10 shows $\langle S^2 \rangle_z$ vs. [NaCl] for all three polyelectrolytes. All show very rapid decreases up to a few mM, after which xanthan levels off, as it also did for A_2, but HA and PSS continue to decrease.

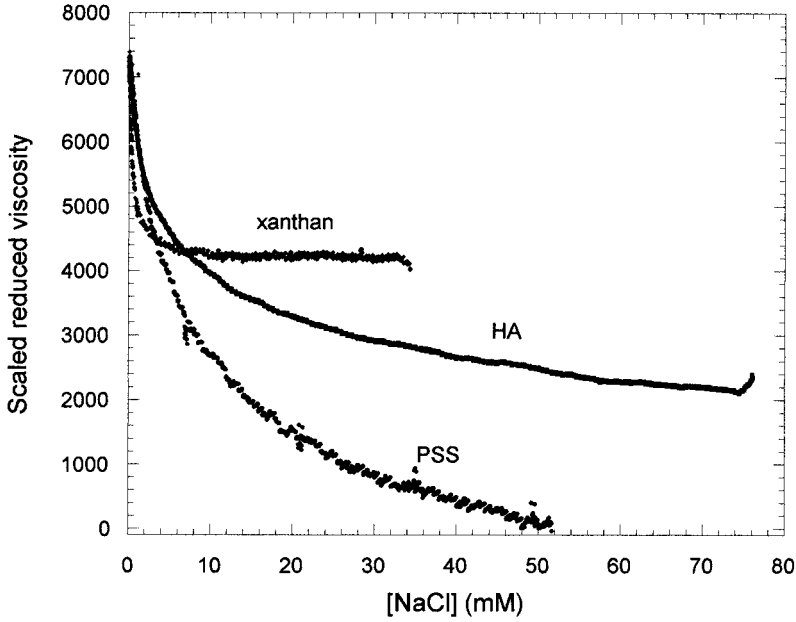

FIGURE 6 Reduced viscosities for poly(styrenesulfonate), hyaluronic acid and xanthan on a single curve, scaled to a single value.

Figure 11 shows $\langle S^2 \rangle_z$ vs. 1/sqrt([NaCl]) for PSS. The trend is fairly linear from high salt down to about [NaCl] = 6 mM. This representation was chosen because it has been previously shown, using experimental data, by Monte Carlo simulations[9], and by combining electrostatic excluded volume and persistence length theories[8,9,11] that such an approximate dependence exists over moderate ranges of ionic strength (usually cited as between 1 mM and 1 M).

The departure from the 1/sqrt(c_s) behavior at very low ionic strength may be due to several factors, including breakdown of the assumptions behind the theories. For HA the trend is again linear at moderate salt concentrations. The value at [NaCl] = 100 mM (1/sqrt(c_s) = 0.1) yields $\langle S^2 \rangle_z^{1/2} = 1440$ Å, which is in excellent agreement with the value of 1400 Å, for the same quantity, as measured by SEC, in Table I. This leads to an apparent intrinsic persistence length of 150 Å, which is in fair agreement with the value reported in Reference [34]. If the asymptotic value for the Debye function of 2 is taken, the apparent intrinsic persistence length is 100 Å.

Xanthan yields 1568 Å at infinite c_s, which is also in reasonable agreement with the SEC value. Using the mass/length of 200 g/mol-Å

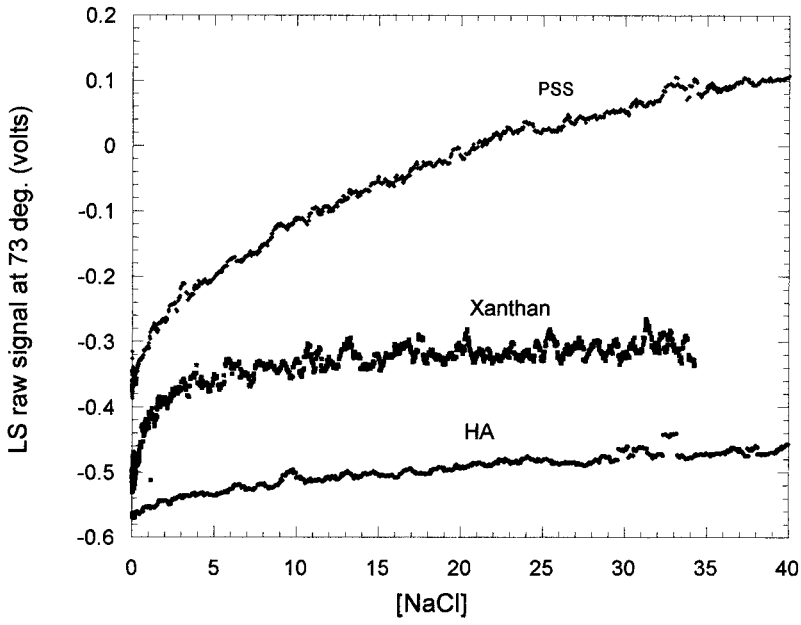

FIGURE 7 Raw light scattering at 73° for the three polyelectrolytes on one graph.

yields an apparent intrinsic persistence length of 1080 Å, also in agreement with the results of Reference [33], and again demonstrates the remarkable stiffness of xanthan, even when fully shielded. This is comparable with the intrinsic stiffness of DNA. At very low ionic strengths (but high enough that the strong interparticle correlations discussed below are shielded), the apparent persistence length is 3820 Å.

The general trend of both viscosity and $\langle S^2 \rangle$ falling off more rapidly and more quickly reaching a high plateau than in more flexible molecules follows from basic considerations. For stiff molecules distant segments cannot approach each other as closely on the average as can distant segments for highly flexible molecules. Hence, the long-range interactions leading to excluded volume effects are screened out at longer range, i.e., at lower ionic strength, for the stiff molecules, and so they reach their minimum $\langle S^2 \rangle$ at lower ionic strength than do flexible polyelectrolytes. The higher plateau for the stiffer molecules simply indicates that, because of the high intrinsic persistence lengths, the fully screened value of $\langle S^2 \rangle$ is still large compared to that of flexible polyelectrolytes (i.e., small intrinsic persistence lengths) that can collapse much further as ionic screening increases.

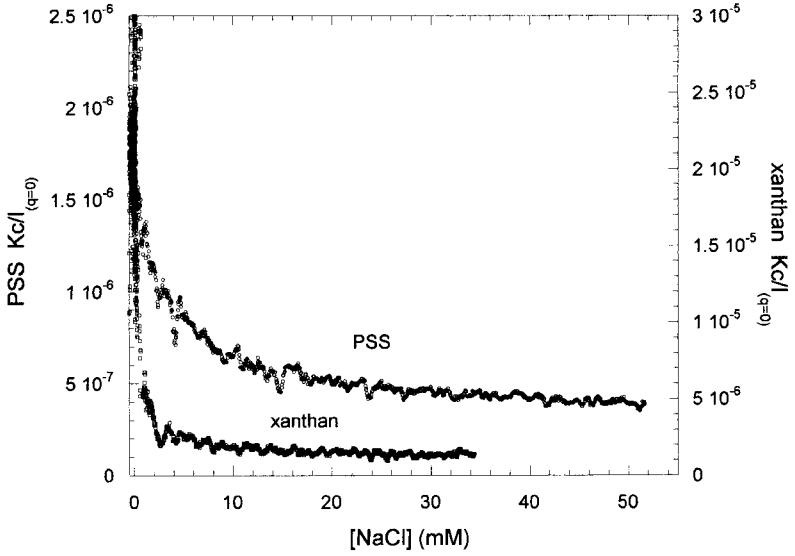

FIGURE 8 $Kc/I(q = 0)$ vs. [NaCl] for the xanthan and poly(styrenesulfonate).

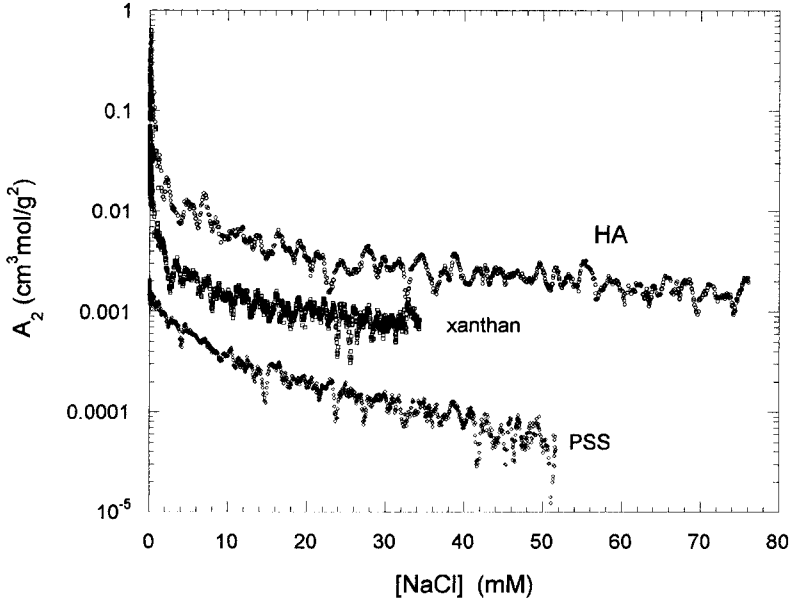

FIGURE 9 A_2 vs. [NaCl] for hyaluronic acid, xanthan and poly(styrenesulfonate).

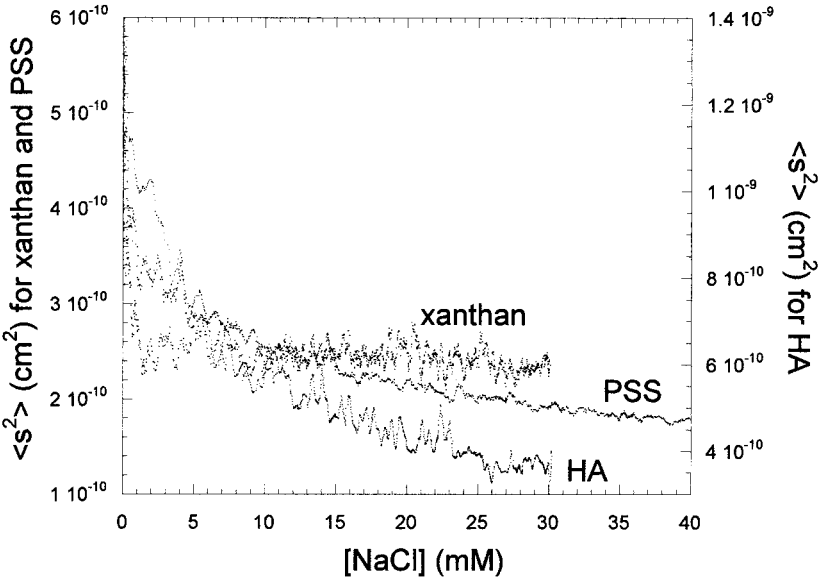

FIGURE 10 $\langle S^2 \rangle_z$ vs. [NaCl] for the three polyelectrolytes.

Xanthan presents an interesting scattering case at low ionic strength. Figure 12 shows that Kc/I vs. q^2 has a negative slope at [NaCl] = 0 and up to over [NaCl] = 0.1 mM. At higher [NaCl], the slope becomes positive, as for a normal polymer solution where scattering from individual polymers dominates the scattering. The negative slope is a manifestation of strong interpolymer correlations at very low ionic strength. This effect has been investigated for xanthan in detail[37]. and reported for several other polyelectrolytes. At high values of q, or lower values of xanthan concentration, the scattering reaches a broad maximum, reminiscent of Bragg scattering peaks[37]. The fact that the negative slopes occur under shear in the flow system argues against there being any long-range order or "crystal structuring" for the xanthan at low ionic strength. A satisfactory analysis in terms of a quasiperiodic, highly damped interparticle potential was given in Reference [37]. Negative slopes and broad maximums have also been observed under shear flow for PSS and proteoglycan subunits[19].

Figure 13 shows reduced viscosity vs. $\langle S^2 \rangle^{3/2}$ for PSS. The plot is quite linear. Intrinsic viscosity $[\eta]$ is related to polymer molecular mass M and hydrodynamic volume V_H, which is in turn related to the hydrodynamic radius by

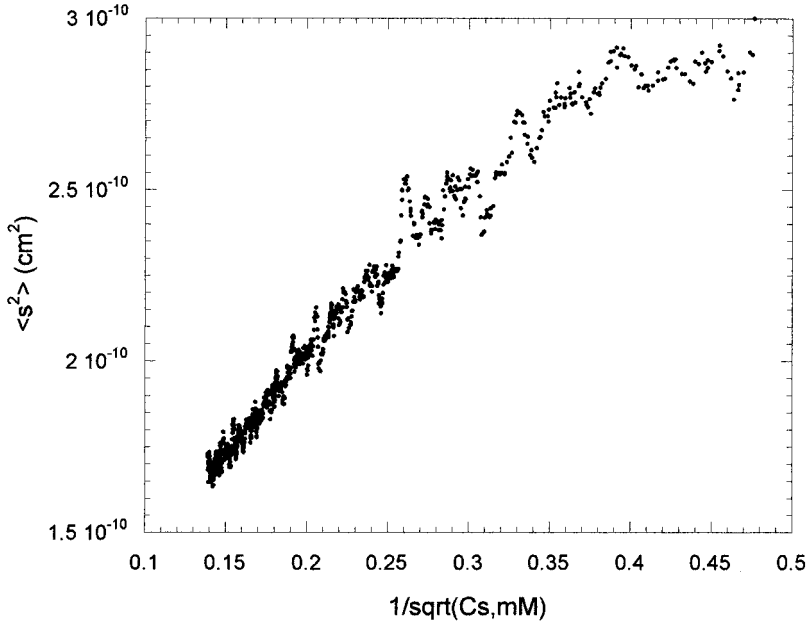

FIGURE 11 $\langle S^2 \rangle_z$ vs. 1/sqrt(c_s) for poly(styrenesulfonate).

$$[\eta] = \frac{V_H N_A}{M} = \frac{4\pi {R_H}^3 N_A}{3M} \tag{11}$$

It is often assumed that R_H is proportional to $\langle S^2 \rangle^{1/2}$ in the so-called nondraining limit for a random coil[38]

$$R_H = \alpha \langle S^2 \rangle^{1/2} \tag{12}$$

where α is approximately 1.37 in this limit. While this has usually been observed for neutral and organosoluble polymers, there have been notable exceptions in the case of polyelectrolytes[35, 39–41]. In this case, however, the linearity in Figure 13 suggests that equation (12) holds, and α can be estimated from

$$\alpha^3 = \frac{3M}{4\pi N_A} \frac{\partial [\eta]}{\partial \langle S^2 \rangle^{3/2}} \tag{13}$$

Using the slope of $1.314 \times 10^{18}\ \mathrm{g}^{-1}$ from Figure 13, and $M = 2.85 \times 10^6$, leads to $\alpha = 1.15$. While this is not quite the result of 1.4 for an ideal,

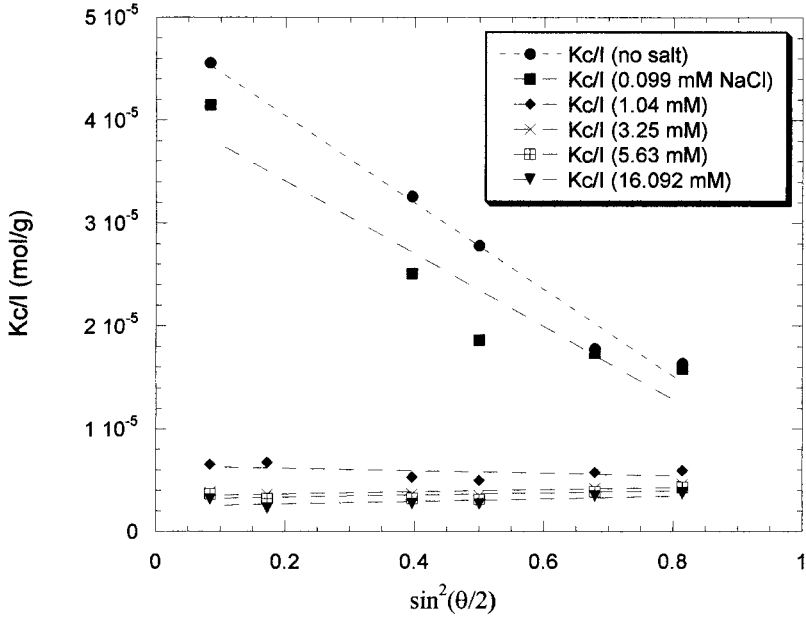

FIGURE 12 Kc/I data for xanthan at very low ionic strengths.

nondraining coil, it is still remarkably close. Since η_r is used in place of $[\eta]$, α may be somewhat overestimated. However, use of the z-average, $\langle S^2 \rangle_z^{3/2}$ and the weight averaged η_r measured by the viscometer will lead to an underestimate. These two errors are therefore at least partially self-canceling. There may also be systematic error in $\langle S^2 \rangle_z^{3/2}$ due to light scattering normalization effects. Finally, polyelectrolytes often deviate markedly from idealized predictions for ideal random coils in theta solvents. At any rate, the ability to cross-correlate independent measures of polymer size and viscosity in a single automatic dilution experiment should open fertile ground for critical assessment of polymer theories.

SUMMARY

A continuous, automatic dilution technique has been introduced to assess the effect of changing solvent conditions on polyelectrolyte properties. The technique was demonstrated with flexible, semiflexible and semirigid polyelectrolytes. The degree of flexibility is immediately apparent from the raw light scattering and viscosity data. The expected trends for viscosity, light scattering, virial coefficients, and radius of

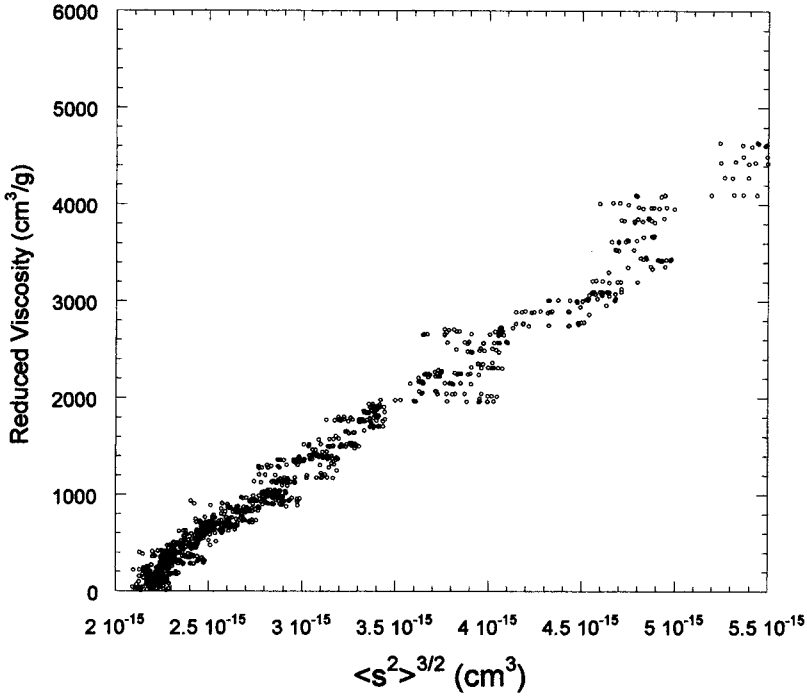

FIGURE 13 Reduced viscosity vs. $\langle S^2 \rangle^{3/2}$ for poly(styrenesulfonate). The linearity is discussed in the text.

gyration were all found in agreement with previous work and theories. All variations in properties were smooth, i.e., no identifiable phase transitions occur for the polyelectrolytes as ionic strength increases. Very strong interparticle correlation effects could be observed in the case of xanthan at very low ionic strength.

Currently, we are refining the experimental portion of the data gathering for higher resolution data, from which quantitative comparisons with theory will be more accurate. The technique will also be applied to continuous polyelectrolyte concentration variation at discrete ionic strengths to determine electrostatic behavior of A_3, for which some theoretical work exists. Studies of continuously varying mixed solvent composition and counter-ion type are likewise planned. It is hoped that the technique will prove valuable for rapidly and accurately assessing the properties of both new and well-known polyelectrolytes. It should also be valuable for determining phase transition behavior for proteins and other polymers.

REFERENCES

[1] Odijk, T. J. (1997). *Polym. Sci. Polym. Phys. Ed.*, **15**, 477.
[2] Odijk, T. J. and Houwaart, A. C. (1978). *Polym. Sci. Polym. Phys. Ed.*, **16**, 627.
[3] Skolnick, J. and Fixman, M. (1977). *Macromolecules*, **10**, 944.
[4] Fixman, M. and Skolnick, J. (1978). *Macromolecules*, **11**, 863.
[5] Dunweg, B., Stevens, M. J. and Kermer, K. (1994). In *Monte Carlo and Molecular Dynamic Simulations in Polymer Science*, ed. K. Binder, Oxford University Press, New York.
[6] Christos, G. A. and Carnie, S. L. (1990). *J. Chem. Phys.*, **92**, 7661.
[7] Brender, C. and Danino, M. (1992). *J. Chem. Phys.*, **97**, 2119.
[8] Reed, C. E. and Reed, W. F. (1990). *J. Chem. Phys.*, **92**(11), 6916.
[9] Reed, C. E. and Reed, W. F. (1991). *J. Chem. Phys.*, **94**(12), 8479.
[10] Förster, S. and Schmidt, M. (1995). *Advt. Polym. Sci.*, **120**, 51.
[11] Reed, W. F. (1994). In *Macroion Characterization. ACS Symp. Ser. 548*, 297–314.
[12] Fuoss, R. M. and Strauss, V. P. (1948). *J. Polym. Sci.*, **3**, 602.
[13] Basu, S. (1951). *Nature*, **168**, 341.
[14] Rinaudo, M., Milas, M., Jouon, M. and Borsali, R. (1993). *Polymer*, **34**, 3710.
[15] Hodgson, D. F. and Amis, E. J. (1991). *J. Chem. Phys.*, **94**, 4581.
[16] Nierlich, M., Williams, C. E., Boue, F., Cotton, J. P., Daoud, M., Farnoux, B., Jannink, G., Picot, C., Moan, M., Wolff, C., Rinaudo, M. and de Gennes, P. G. (1979). *J. Phys.* (Paris), **40**, 701.
[17] Drifford, M. and Dalbiez, J. P. (1984). *J. Phys. Chem.*, **88**, 5368.
[18] Wang, L. and Bloomfield, V. (1991). *Macromolecules*, **24**, 5791.
[19] Li, X. and Reed, W. F. (1991). *J. Chem. Phys.*, **94**, 4568.
[20] Lin, S., Lee, W. I. and Schurr, J. M. (1978). *Biopolymers*, **17**, 1041.
[21] Sedlak, M. and Amis, E. J. (1992). *J. Chem. Phys.*, **96**, 817.
[22] Sedlak, M. (1993). *Macromolecules*, **26**, 1158.
[23] Ghosh, S., Peitzsch, R. M. and Reed, W. F. (1992). *Macromolecules*, **32**, 1105.
[24] Smits, R. G., Kuil, M. E. and Mandel, M. (1994). *Macromolecules*, **27**, 5599.
[25] Morfin, I., Reed, W. F., Rinaudo, M. and Borsali, R. (1994). *J. Phys. II* (France), **4**, 1001.
[26] Michel, R. C. and Reed, W. F. (2000). *Biopolymers*, **53**, 19.
[27] Florenzano, F. H., Strelitzki, R. and Reed, W. F. (1998). *Macromolecules*, **31**, 7226.
[28] Strelitzki, R. and Reed, W. F. (1999). *J. Appl. Polym. Sci.*, **73**, 2359.
[29] Norwood, D. P. and Reed, W. F. (1997). *Int. J. Polym. Anal. Charact.*, **4**, 99.
[30] Zimm, B. H. (1948). *J. Chem. Phys.*, **16**, 1093.
[31] Huggings, M. L. (1942). *J. Am. Chem. Soc.*, **64**, 2716.
[32] Reed, W. F. (1996). Ch.2, In *Strategies in Size Exclusion Chromatography*, eds. Dubin and Potschak, ACS, Washington, D.C.
[33] Milas, M., Reed, W. F. and Printz, S. (1996). *Int. J. Biol. Macromole.*, **18**, 211.
[34] Ghosh, S., Li, X., Reed, C. E. and Reed, W. F. (1990). *Biopolymers*, **30**, 1101.
[35] Peitzsch, R. M., Burt, M. J. and Reed, W. F. (1992). *Macromolecules*, **25**, 806.
[36] Benoit, H. and Doty, P. J. (1953). *J. Phys. Chem.*, **57**, 958.
[37] Norwood, D. P., Benmouna, M. and Reed, W. F. (1996). *Macromolecules*, **29**(12), 4293.
[38] Debye, P. (1947). *Phys. Rev.*, **71**, 486.
[39] Kurta, M. and Yamakawa, H. (1958). *J. Chem. Phys.*, **29**, 311.
[40] Weill, G. and des Cloizeaux, J. (1979). *J. Phys.* (Orsay, Fr.), **40**, 99.
[41] Reed, W. F., Ghosh, S., Medjahdi, G. and Francois, J. (1991). *Macromolecules*, **24**, 6189.